Journal of Fluorescence, Vol. 5, No. 1, 1995

Determination of DPH Order Parameters in Unoriented Vesicles

D. Toptygin[1] and L. Brand[1,2]

Received September 27, 1994; accepted September 27, 1994

This article reviews the determination of orientational order parameters in non-macroscopically oriented membranes from the data obtained with the fluorescent probe all-*trans*-1,6-diphenyl-1,3,5-hexatriene (DPH). Special attention is paid to the effect of microheterogeneity in the probe environment on the recovered values of the order parameters. An effort is made to accommodate new findings in the existing picture of orientational order in membranes.

KEY WORDS: Fluorescence; order parameters; lipid membranes; refractive index; microheterogeneity; diphenylhexatriene.

INTRODUCTION

The knowledge of physical characteristics of lipid membranes is of great importance for understanding their biological functions. Fluorescence of hydrophobic probes introduced in the hydrocarbon region of membrane bilayers offers a unique possibility for studying orientational order and dynamics in membranes. Early studies of fluorescence polarization in membranes [1–3] assumed isotropic rotational behavior. Orientational order was not taken into consideration. The Perrin equation [4] was employed to relate the value of the steady-state fluorescence anisotropy to the microviscosity of the probe environment.

When nanosecond time-resolved fluorescence anisotropy data became available [5–7], marked qualitative differences between time-resolved anisotropy $r(t)$ in membranes and in isotropic media were discovered. In isotropic systems, $r(t)$ decayed to zero, while in membranes it decayed to a constant value $r_\infty \neq 0$. The nonzero r_∞ value suggested that probe rotation was not free [6,7]. This was interpreted in terms of the wobbling-in-cone model [7,8] and related to the "degree of orientational constraint" [8]. It was later realized [9–11] that the "degree of orientational constraint" equals the square of the second-rank order parameter $\langle P_2 \rangle$ commonly used in the theory of liquid crystals and in electron spin and nuclear magnetic resonance studies of membranes.

In initial studies [8–11] the behavior of $r(t)$ between the values of r_0 and r_∞ was considered to be approximately exponential. Zannoni *et al.* [12,13] described a model for rotational diffusion in the presence of an effective aligning potential which predicted the exact shape of the function $r(t)$. The function $r(t)$ was approximated by a sum of exponentials [14]. The preexponential factors and depolarization rates were related to the values of the order parameters $\langle P_2 \rangle$ and $\langle P_4 \rangle$. Fits of experimental data to the sum of exponential terms allowed the determination of the order parameter $\langle P_4 \rangle$ [15,16]. In the determination of the fourth-rank order parameter the membrane was implicitly assumed to be homogeneous: the rotational diffusion rate was assumed to have one value in all parts of the membrane bilayer.

The possible influence of heterogeneity in the location of the probe was considered in early studies [5,6].

[1] McCollum-Pratt Institute, Department of Biology, Johns Hopkins University, Baltimore, Maryland 21218.

[2] To whom correspondence should be addressed.

1053–0509/95/0300–0039$07.50/0

Attempts to "associate" individual fluorescence intensity decay times with emission anisotropy decay components did not lead to physically realistic solutions [6]. The notion of multiple environments was also tested with the aid of emission-anisotropy-decay-associated spectroscopy [17]. In this case an association between spectral distribution and anisotropy was found.

Theory predicts [12,13] that in general the time-resolved fluorescence anisotropy of a probe in an anisotropic environment will be complex. The problem is simplified in the case of a rodlike fluorescent probe having its absorption and emission dipoles parallel or near-parallel to the rod axis. All-*trans*-1,6-diphenyl-1,3,5-hexatriene (DPH) represents a good example of such a probe [3,18] and has been one of the most popular membrane probes [19]. Lentz [20,21] has reviewed the use of DPH and other fluorescent probes to monitor molecular order and motion within liposome bilayers.

While the rotational properties of DPH are convenient for fluorescence anisotropy studies, other characteristics of this probe are quite unusual. The natural lifetime of DPH was found to be sensitive to its environment [22,23]. The absorption and emission spectra of this probe have no mirror symmetry. The absorptivity and natural lifetime do not satisfy the relation of Strickler and Berg [24]. Several hypotheses have been proposed to account for the unusual characteristics of DPH [25–28]. These hypotheses are not directly related to membrane studies except for the fact that the environmental sensitivity of DPH must be taken into consideration in these studies.

The theory of fluorescence depolarization in membranes [12,13] assumed that the total fluorescence intensity decay is exponential. The intensity decay of DPH was found to be exponential in homogeneous liquid solvents [23], but not in membranes [5–7]. Multiexponential fluorescence decay of DPH in membranes could result from the heterogeneity of its environment. The multiexponential decay has been associated with domain structure [29–31]. However, it was found that the fluorescence intensity decay of DPH in membranes that do not form domain structure is also multiexponential [31–34]. This was interpreted in terms of complex photochemistry [33] or photophysics [34] of DPH.

An alternative explanation for the nonexponential fluorescence decay of DPH in membranes has been proposed [35,36]. This is based on the electromagnetic characteristics of membranes. A lipid membrane may be described as a thin film of one refractive index surrounded by a medium of another refractive index. The emission of electromagnetic waves in such a system was theoretically studied by Lukosz [37]. It was shown that the radiative decay rate in a thin film depends on the orientation of the emitting dipole with respect to the membrane. The early theory of fluorescence depolarization in membranes [9–14] did not take into account the orientational dependence of the radiative decay rate. When the effect of this orientational dependence is taken into account, nonexponential total fluorescence intensity and anisotropy decays are expected [35,36]. This model allows the determination of several interesting parameters, including the refractive index inside the bilayer. It was determined that the orientational dependence of the radiative decay rate can account for the broad spectrum of DPH decay times in membranes if the refractive index in the hydrocarbon region of the bilayer exceeds the refractive index of water by approximately 20% [36] or 25% [35].

The refractive index inside a bilayer was recently measured by a more straightforward technique [38]. This refractive index proved to be 1.425, which is only 7% greater than the refractive index of water. With the lower value of the refractive index the orientational dependence of the radiative decay rate cannot account for the broad spectrum of DPH decay times in membranes. This implies that the orientational dependence of the radiative decay rate may not be the only process that contributes to the complex decay of DPH in membranes. The lifetime of DPH depends on the solvent environment [23]. The heterogeneity of the bilayer interior may well contribute to the width of DPH lifetime spectrum. Gratton and Parasassi [39] suggested that the concentration of water in the hydrocarbon region of the bilayer can play the role of the factor that modulates the lifetime of DPH.

The theory developed by Lukosz [37] and applied to membranes by Toptygin and Brand [38] predicts the dependence of the radiative decay rate on the refractive index of the medium surrounding the membrane. The variation in the radiative decay rate of DPH in liposomes with changes in the external refractive index was used to recover the order parameter $\langle P_2 \rangle$. The value obtained differs from that derived from emission anisotropy data for reasons that are not yet clear.

In the present paper we review the concept of orientational order parameters in membranes and discuss the possible effects of microheterogeneity in probe environment on the recovered values for the order parameters.

REVIEW OF BASIC CONCEPTS

Definition of Orientational Order Parameters

The orientation of a rodlike fluorescent probe having absorption and emission dipoles parallel to the rod

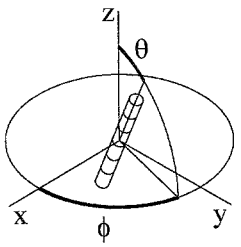

Fig. 1. Description of the orientation of a rodlike probe by the spherical angles θ and ϕ.

axis can be completely described by the spherical angles θ and ϕ shown in Fig. 1. Here θ is the angle between the Z axis and the rod axis, whereas ϕ is the angle between the X axis and the projection of the rod axis on the XY plane. The orientational distribution of the probe is characterized by the function $f(\theta,\phi)$, which represents the density of probability of finding the probe molecule at a certain orientation.

Although the detailed form of the orientational distribution function cannot be determined from experimental data, some characteristics of this function can be recovered. Experimentally measurable quantities represent averages over all orientations of the probe. If a quantity A depends on the orientation of the probe, then the mean value of this quantity is given by the equation

$$\langle A \rangle = \int_0^{\pi} \int_0^{2\pi} A(\theta,\phi) f(\theta,\phi) \sin\theta \, d\theta \, d\phi \qquad (1)$$

Here we have assumed that the orientational distribution function is normalized by the relation

$$\int_0^{\pi} \int_0^{2\pi} f(\theta,\phi) \sin\theta \, d\theta \, d\phi = 1 \qquad (2)$$

Orientational dependences of most physical quantities, such as the probabilities of fluorescence excitation or emission, can be expressed in terms of the Legendre polynomials $P_L(\cos\theta)$, where $L = 0,1,2,\ldots$. This enables one to measure the mean values, $\langle P_L(\cos\theta)\rangle$. These mean values are called the orientational order parameters.

Knowledge of the order parameters is sometimes sufficient to reconstruct the orientational distribution function. What is even more important, the outcome of most experiments can be predicted on the basis of the values of a few order parameters, without knowing the detailed form of the orientational distribution function.

If the probe molecule has a center of symmetry, then none of the measurable physical quantities will depend on the Legendre polynomials of the odd powers L. Most of the quantities can be expressed in terms of the first few even-power polynomials. Here we will consider the first three: $P_0(\cos\theta) = 1$, $P_2(\cos\theta) = (3\cos^2\theta - 1)/2$, $P_4(\cos\theta) = (35\cos^4\theta - 30\cos^2\theta + 3)/8$. The mean values of the physical quantities can be expressed in terms of the corresponding order parameters. The order parameter $\langle P_0(\cos\theta)\rangle$ always equals unity, and therefore it does not need to be measured. The values of the order parameters $\langle P_2(\cos\theta)\rangle$ and $\langle P_4(\cos\theta)\rangle$ equal zero when the orientational distribution is isotropic. In an anisotropic environment, such as a lipid membrane, the values of these parameters can be determined experimentally using different fluorescence techniques.

Orientation of the Director

It is clear that the form of the orientational distribution function $f(\theta,\phi)$ and the values of the order parameters $\langle P_L(\cos\theta)\rangle$ depend on the choice of the XYZ frame. In macroscopically unoriented suspensions of lipid membranes the orientation of molecules with respect to the laboratory frame will appear random even though the orientation of the molecules with respect to the membrane is not random. We are interested in studying the orientation of molecules with respect to the membrane; therefore a separate XYZ frame should be associated with every membrane fragment. It is traditional to take the direction normal to the surface of the membrane bilayer for the Z axis [8,9]. The membrane appears to be symmetrical with respect to the rotations around this axis; therefore it is likely that the orientational distribution of the probe also will be symmetrical with respect to this axis. On the other hand, it is sometimes assumed that the lipid acyl chains are tilted at a certain angle [40–42]. In this case it is more reasonable to expect that the orientational distribution will be symmetrical with respect to some tilted axis Z'. It is also possible that the orientational distribution has no symmetry axis at all.

From the fluorescence data obtained with macroscopically unoriented suspensions of lipid membranes one cannot determine whether the orientational distribution has a symmetry axis nor the orientation of this axis with respect to the membrane bilayer. As a compromise we can assume that the orientational distribution of the fluorescent probe is approximately symmetrical with respect to some axis Z', which will be referred to as the director. The director may coincide or not coincide with the axis Z, which represents the normal to the membrane surface. The spherical angles measured in the $X'Y'Z'$ frame will be designated θ', ϕ', whereas the spher-

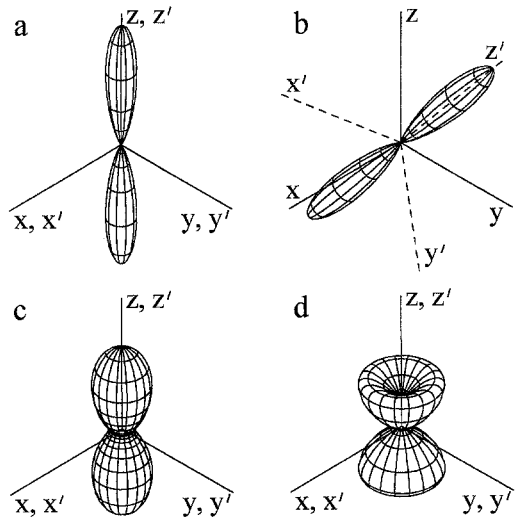

Fig. 2. Examples of hypothetical orientational distributions of a rodlike probe in a membrane. The Z axis is normal to the membrane surface. The length of the radius vector drawn from the origin to a point on the three-dimensional surface represents the density of probability of finding the probe at the orientation parallel to the radius vector. The values of the order parameters are (a) $\langle P_2(\cos\theta)\rangle = \langle P_2(\cos\theta')\rangle = 0.9$, $\langle P_4(\cos\theta')\rangle = 0.7$; (b) $\langle P_2(\cos\theta)\rangle = 0.3$, $\langle P_2(\cos\theta')\rangle = 0.9$, $\langle P_4(\cos\theta')\rangle = 0.7$; (c) $\langle P_2(\cos\theta)\rangle = \langle P_2(\cos\theta')\rangle = 0.3$, $\langle P_4(\cos\theta')\rangle = 0.06$; (d) $\langle P_2(\cos\theta)\rangle = \langle P_2(\cos\theta')\rangle = 0.3$, $\langle P_4(\cos\theta')\rangle = -0.1$.

ical angles in the XYZ frame will be designated θ, ϕ. The existence of two frames assumes two orientational distribution functions $f(\theta', \phi')$ and $f(\theta, \phi)$ and two sets of orientational order parameters $\langle P_L(\cos\theta')\rangle$ and $\langle P_L(\cos\theta)\rangle$.

The orientational distribution in the $X'Y'Z'$ frame is symmetrical with respect to the axis Z'; therefore the function $f'(\theta', \phi')$ does not depend on the angle ϕ'. The shape of this function can be reconstructed from the values of the order parameters using the properties of Legendre polynomials:

$$f'(\theta',\phi') = \sum_{L=0}^{\infty} \frac{2L+1}{4\pi} \langle P_L(\cos\theta')\rangle P_L(\cos\theta') \quad (3)$$

In the hypothetical situation where the director is not normal to the membrane surface, the orientational distribution function is not symmetrical with respect to the rotations around the Z axis and it cannot be reconstructed from the values of the order parameters $\langle P_L(\cos\theta)\rangle$. Rigorously speaking, the mean values $\langle P_L(\cos\theta)\rangle$ should not be called order parameters in this situation. For a complete description of the orientational order in a system with a tilted symmetry axis or without this axis, one needs to employ the Wigner rotation matrices $D^L_{mn}(\phi, \theta, \psi)$ [13] instead of the Legendre polynomials. This approach results in a greater number of unknown order parameters $\langle D^L_{mn}(\phi, \theta, \psi)\rangle$, which cannot be uniquely determined from the experimental data obtained with macroscopically unoriented suspensions of lipid membranes.

Fluorescence techniques capable of measuring the order parameters $\langle P_L(\cos\theta')\rangle$ and $\langle P_L(\cos\theta)\rangle$ will be discussed later, and here we will give a few examples of orientational distributions corresponding to different values of these order parameters. Figure 2 shows orientational distributions for a rodlike molecule such as DPH for a number of different situations.

The orientational distributions shown in Figs. 2a and 2b have identical values of the order parameter $\langle P_2(\cos\theta')\rangle = 0.9$. These orientational distributions are indistinguishable by an experimental technique sensitive only to the order parameters $\langle P_L(\cos\theta')\rangle$, but they can be distinguished by a technique sensitive to the order parameters $\langle P_L(\cos\theta)\rangle$.

The distributions shown in Figs. 2b and 2c have identical values of the order parameter $\langle P_2(\cos\theta)\rangle = 0.3$. These orientational distributions are indistinguishable by an experimental technique sensitive only to the order parameter $\langle P_2(\cos\theta)\rangle$.

Some experimental techniques allow the determination of the fourth-rank order parameter $\langle P_4(\cos\theta')\rangle$. The value of this parameter has a great effect on the shape of the orientational distribution. The orientational distributions shown in Figs. 2a–2c have positive values of the order parameter $\langle P_4(\cos\theta')\rangle$, which correspond to the model of Maier and Saupe (see Zannoni *et al.* [13]), also known as the Gaussian model [14]. Figure 2d represents the orientational distribution with a negative value of $\langle P_4(\cos\theta')\rangle$. Negative values of this order parameter have been reported by Wang *et al.* [16].

In both Figs. 2b and 2d tilted orientations of the fluorescent probe are more frequent than the normal one; however, there is a significant difference between the two cases. In the case shown in Fig. 2b the orientation of the director is tilted. In the case shown in Fig. 2d the orientation of the director is normal to the membrane surface. We may assume that the orientation of the director in a lipid membrane reflects the direction of the acyl chains. If this assumption is correct, then the orientational distribution shown in Fig. 2d represents the situation where the orientation of the acyl chains is normal to the membrane surface, but the axis of the rodlike probe makes the angle about 35° with the acyl chains. In contrast, in Fig. 2b the acyl chains are tilted, and the probe is aligned near-parallel to the acyl chains.

The examples shown in Fig. 2 illustrate the importance of applying alternative experimental techniques to the same sample. The technique capable of measuring

either the parameters $\langle P_L(\cos\theta')\rangle$ or $\langle P_L(\cos\theta)\rangle$ would not be capable of distinguishing between the case of the normal director and that of the tilted director.

THE SECOND-RANK ORDER PARAMETER $\langle P_2\rangle$

Order Parameter $\langle P_2\rangle$ from the Limiting Anisotropy

Fluorescence emission anisotropy r is defined as the ratio $(I_\parallel - I_\perp) / (I_\parallel + 2I_\perp)$, where $I_\parallel$ and $I_\perp$ are the intensities of the polarization components parallel and perpendicular to the polarization of the excitation radiation, respectively. The behavior of the time-resolved fluorescence anisotropy $r(t)$ contains valuable information about orientational order and dynamics.

The limiting anisotropy r_∞ is defined as the limit of the time-resolved anisotropy $r(t)$ at $t \to \infty$. It has been shown both theoretically and experimentally that in isotropic media, r_∞ equals zero. The results obtained with the fluorescent probe DPH in phospholipid vesicles clearly demonstrated that the time-resolved anisotropy does not decay to zero [5–7]. The suspensions of phospholipid vesicles are isotropic on the macroscopic level; however, on the microscopic level the orientational distribution of the fluorescent probe is not isotropic. If we assume that the local orientational distribution has a symmetry axis, i.e., the local director Z, and that the angle θ' is measured with respect to this local director, then the following relation will hold:

$$r_\infty = r_0 \langle P_2(\cos\theta')\rangle^2 \tag{4}$$

In Eq. (4), r_0 is the value of $r(t)$ at $t = 0$. For a fluorescent probe having parallel absorption and emission dipoles $r_0 = 0.4$. Equation (4) has been derived by several authors [8–13]. It is of interest to review the main assumptions implicit in Eq. (4). The first is that the local orientational distribution is symmetrical with respect to the local director from which the angle θ' is measured. The second is that the local directors are randomly oriented on the macroscopic level. The orientation of the local director with respect to the membrane normal is not critical. Equation (4) holds true whether the director is normal to the surface or tilted; it holds true even in the case where the orientation of the local director is individual for every probe molecule. This is true since the fluorescence anisotropy monitors the reorientation of the probe molecule rather than the absolute orientation of this molecule with respect to the membrane bilayer. Consequently, anisotropy decay depends on the order parameters $\langle P_L(\cos\theta')\rangle$ rather than $\langle P_L(\cos\theta)\rangle$. Equation (4) can be used to recover the order parameter $\langle P_2(\cos\theta')\rangle$.

An important question associated with the use of Eq. (4) concerns the possibility of determining r_∞ from experimental data. The decay of $r(t)$ between r_0 and r_∞ may contain one or several exponentials, depending on the mechanism of orientational dynamics. For DPH, in a homogeneous liquid-crystalline membrane all of the anisotropy decay components are probably faster than the fluorescence intensity decay; therefore, by the time fluorescence intensity becomes too low to be measured, the time-resolved anisotropy approximates the value of r_∞. In heterogeneous or gel-phase membranes some of the anisotropy decay components can be slower than the intensity decay. In this case the value of the limiting anisotropy determined from the anisotropy decay data is not the r_∞ involved in Eq. (4).

The problem in measuring r_∞ can be illustrated with the case of a solution of DPH in pure glycerol. Since this is an isotropic solution, we know *a priori* that $r_\infty = 0$. On the other hand, in the time-resolved anisotropy data obtained with this sample one will not be able to see $r(t)$ approaching zero. This occurs because the rotational diffusion in glycerol is much slower than the intensity decay. Phospholipid molecules are bulkier than the glycerol molecules. It is possible that in a gel-phase phospholipid membrane some of the rotational diffusion components are slower than in glycerol. In this case the order parameters calculated from Eq. (4) for mixed- and gel-phase membranes may be exaggerated significantly.

As an example, consider a hypothetical heterogeneous membrane having two kinds of environments, the first one being glycerol-like and containing 80% of DPH molecules, and the second one being liquid in character and containing 20% of DPH. If the value of the actual order parameter $\langle P_2(\cos\theta')\rangle$ equals 0.3 in every environment, then the apparent value of r_∞ equals $0.4 \times (0.8 + 0.2 \times 0.3^2) = 0.33$, and the value of $\langle P_2(\cos\theta')\rangle$ recovered from Eq. (4) equals 0.9.

Correcting $\langle P_2\rangle$ Obtained from the Limiting Anisotropy for the Refraction of Light at the Lipid–Water Interface

In membranes which are free from the gel phase the order parameter $\langle P_2(\cos\theta')\rangle$ can be reliably determined from the value of the limiting anisotropy. Equation (4), which links the values of r_∞ and $\langle P_2(\cos\theta')\rangle$, has been derived under the assumption that the fluorescent probe interacts with the macroscopic electromagnetic field of the light wave. The local electromagnetic field of the light wave inside the membrane differs from

the macroscopic field in both magnitude and direction of the electric vector. The influence of this difference on the fluorescence depolarization was considered in Refs. 35 and 36 under the explicit assumption that the orientation of the director is normal to the membrane surface. The results obtained in that work are not valid for the hypothetical situation where the axes Z' and Z do not coincide. If the director is normal to the membrane surface, then $\theta' = \theta$, which makes it possible to use the short form $\langle P_2 \rangle$ instead of both $\langle P_2(\cos \theta') \rangle$ and $\langle P_2(\cos \theta) \rangle$.

Because of the difference between the local electromagnetic field and the macroscopic field, the decays of the fluorescence total intensity and anisotropy are not independent. The initial orientational distribution of the excited probe may not relax to the stationary orientational distribution function because the probe molecules oriented normal to the membrane surface lose excitation slower than those deviating from the normal orientation. However, if the rotational relaxation is much faster than the intensity decay, then the orientational distribution of the excited probe at long times after the excitation will closely approximate the stationary distribution. In this case one can derive a simple relation between the values of r_∞ and $\langle P_2 \rangle$. This relation can be found in Eq. (24) in Ref. 35. For simplicity we can replace the ratio of the constants a^2/b^2 used in Ref. 35 with $(n_1/n_0)^4$, where n_0 and n_1 are the refractive indices of water and the bilayer interior, respectively. After this substitution the equation becomes

$$r_\infty = 0.4 \frac{[-n_1^4/n_0^4+1+(n_1^4/n_0^4+2)\langle P \rangle]^2}{[2n_1^4/n_0^4+1-2(n_1^4/n_0^4-1)\langle P_2 \rangle]^2} \qquad (5)$$

Equation (5) is valid only if the director is normal to the membrane surface, absorption and emission dipoles are parallel to the axis of a rodlike fluorescent probe, and the rotation is much faster than the intensity decay. When the refractive index of the bilayer interior coincides with that of water and $r_0 = 0.4$, Eq. (5) reduces to Eq. (4).

The refractive index of the bilayer interior is only slightly greater than that of water. In Ref. 38 the value of $n_1 = 1.425$ was obtained for DPPC at 20°C, whereas $n_0 = 1.333$. This results in $(n_1/n_0)^4 \approx 1.3$. Using the latter ratio, we can recover the value of $\langle P_2 \rangle$ for a typical value of r_∞. The value of r_∞ for DPH in DPPC at 55°C is close to 0.036 [36]. Substituting this value in Eq. (4) would yield $\langle P_2 \rangle = +0.3$ and $\langle P_2 \rangle = -0.3$. The negative value of $\langle P_2 \rangle$ is usually disregarded because it makes no sense. Equation (5) also yields two solutions: $\langle P_2 \rangle = +0.397$ and $\langle P_2 \rangle = -0.25$. Again, the negative value can be disregarded, and the positive value is only slightly different than that obtained from Eq. (4).

The above example shows that the refraction of light at the lipid–water interface results in a small correction to the value of the order parameter $\langle P_2 \rangle$ obtained from Eq. (4).

Determination of the Order Parameter $\langle P_2 \rangle$ from the Effect of Refractive Index Changes

The fluorescence lifetime is the inverse of the sum of the radiative and nonradiative decay rates,

$$\tau = \frac{1}{k_r + k_{nr}} \qquad (6)$$

The radiative and nonradiative rates can be calculated as

$$k_r = \eta/\tau, \qquad k_{nr} = (1-\eta)/\tau \qquad (7)$$

where η is the quantum yield. The radiative rate depends on the intrinsic properties of the fluorescent probe and on the optical characteristics of the probe environment. The most fundamental optical characteristic of a homogeneous medium is its refractive index. In a heterogeneous environment one needs to take into account the spatial variations in the refractive index. Local variations in the refractive index may have a significant effect on the radiative decay rate only if they occur at a distance of less than the light wavelength from the fluorescent probe.

The peak wavelength of DPH fluorescence is about 425 nm, whereas the thickness of the membrane bilayer is about 5–7 nm. The refractive index of the membrane interior is different than that of water. The local variations of the refractive index take place at a distance much less than the light wavelength, therefore they should affect the radiative decay rate.

In general, the radiative rate will depend not only on the refractive indexes inside and outside the membrane, but also on the shape of the membrane and on the position and orientation of the fluorescent probe with respect to the membrane. Phospholipid membranes may assume different shapes. The radiative rate can be easily predicted for DPH in large unilamellar vesicles (LUVs). The diameter of an LUV is large compared to the thickness of its walls, therefore the membrane bilayer that forms the LUV can be treated as an isolated flat film of one refractive index immersed in a medium of another refractive index.

Lukosz considered the radiation of a classical dipole located inside an optically thin film [37]. He showed that the radiative rate for the dipole oriented

normal to the surface of the film is proportional to the fifth power of the external refractive index, whereas the decay rate for the dipole oriented parallel to the surface is proportional to the first power of the external refractive index. The same result was derived from quantum mechanical principles [38]. The radiative rate was also predicted for any intermediate orientation of the emission dipole. This is given by

$$k_r = \frac{4\omega^3}{3\hbar c^3} f^2 |\boldsymbol{\mu}|^2 n_0 (\sin^2\theta + \frac{n_0^4}{n_1^4}\cos^2\theta) \quad (8)$$

where ω is the circular frequency of fluorescence light, $\hbar$ is Planck's constant, c is the speed of light in vacuum, f is the factor that accounts for the difference between the local electric field experienced by the probe and the macroscopic field inside the membrane, $\boldsymbol{\mu}$ is the matrix element of the electric dipole operator (emission dipole), n_1 and n_0 are the refractive indexes of the layer and the surrounding medium, respectively, and θ is the angle between the emission dipole and the normal to the surface of the membrane bilayer.

The radiative rate from Eq. (8) is different for different orientations of the probe molecule. If the probe can assume different orientations, then the total fluorescence intensity decay will be nonexponential. The ratio of the longest and the shortest lifetimes does not exceed $(n_1/n_0)^4$. The difference between the refractive indexes of lipid and water is less than 10%; therefore the ratio of the longest and the shortest lifetimes will be less than 1.5. When the lifetimes are so close, their values cannot be measured separately, but the mean lifetime can be still measured with great accuracy. The mean lifetime is defined as

$$\bar{\tau} = \int_0^\infty tI(t)\,dt \Big/ \int_0^\infty I(t)\,dt = \frac{\sum \alpha_n \tau_n^2}{\sum \alpha_n \tau_n} \quad (9)$$

where $I(t)$ is the δ-excitation total fluorescence intensity decay, and α_n and τ_n are the preexponential factors and lifetimes, respectively, for individual exponentials recovered in the analysis of decay data. It has been shown [38] that the behavior of this mean lifetime with change in refractive index can be approximated by

$$\frac{1}{\bar{\tau}} = k_{nr} + \gamma(1 - \langle P_2(\cos\theta)\rangle) n_0 + \gamma n_1^{-4} (\langle P_2(\cos\theta)\rangle + \frac{1}{2}) n_0^5 \quad (10)$$

where γ is the combination of several constants from Eq. (8), and the error of the approximation is less than 0.3% for a high-quantum-yield probe like DPH.

The value of the order parameter $\langle P_2(\cos\theta)\rangle$ can be determined from the lifetime variation with the refractive index. Equation (10) can be linearized in the following way:

$$\begin{aligned} y &= Ax + B \\ x &= n_0^4 \\ y &= (1/\bar{\tau} - k_{nr})/n_0 \end{aligned} \quad (11)$$

Coefficients A and B can be determined from a linear plot and/or by linear regression. The order parameter can be calculated according to

$$\langle P_2(\cos\theta)\rangle = \frac{An_1^4 - \frac{1}{2}B}{An_1^4 + B} \quad (12)$$

A technique for measuring the value of n_1 that needs to be substituted in Eq. (12) is described in [38].

In the analysis of the lifetime dependence on the refractive index it was assumed that the values of the parameters γ, n_1, k_{nr}, and $\langle P_2(\cos\theta)\rangle$ do not change when the refractive index of the medium surrounding the bilayers is varied. As the values of these parameters depend on the physical characteristics of the bilayer interior, they should not directly depend on the chemical composition of the surrounding medium unless the changes in this medium affect the bilayer.

In Ref. 38 the refractive index n_0 was varied by the addition of either glycerol or sucrose to the aqueous solutions used in the preparation of the large unilamellar vesicles. The data obtained with both additives fall on the same line in the linearized coordinates given by Eq. (11). This suggests that glycerol and sucrose influence the fluorescence by the refractive index effect rather than by an indirect effect on the structure of the bilayer. It is also possible that both glycerol and sucrose influence the structure of the bilayer and the experimental points obtained with these additives fall on the same line by coincidence. This could lead to an error in the determination of the order parameter.

Comparison of $\langle P_2\rangle$ Values Obtained by Different Techniques

The experiments involving the variation of the refractive index of the solution used in the preparation of large unilamellar vesicles yielded $\langle P_2(\cos\theta)\rangle = 0.285$ for DPH in DPPC at 20°C [38]. The apparent value of r_∞ obtained for the same sample at the same conditions equals 0.33. If $r_0 = 0.4$, then from Eq. (4) one can obtain $\langle P_2(\cos\theta')\rangle = 0.91$. A lower value for r_0 would result in an even higher value for $\langle P_2(\cos\theta')\rangle$. Here we face

the situation where the value of $\langle P_2(\cos\theta)\rangle$ obtained by one technique and the value of $\langle P_2(\cos\theta')\rangle$ obtained by the other technique are far away from each other. There are at least two possible explanations of this result.

The first possibility is that the director axis Z' is tilted with respect to the bilayer normal as shown in Fig. 2b. The angle θ'' between the axes Z' and Z can be calculated:

$$\theta'' = \arccos\left\{\left[\frac{2\langle P_2(\cos\theta)\rangle}{3\langle P_2(\cos\theta')\rangle} + \frac{1}{3}\right]^{1/2}\right\} \quad (13)$$

Estimation of θ'' based on Eq. (13) gives a value $\theta'' = 43°$. The director of the orientational distribution shown in Fig. 2b is tilted by this angle and the values of the order parameters $\langle P_2(\cos\theta)\rangle$ and $\langle P_2(\cos\theta')\rangle$ for the orientational distribution are close to those determined by variation of the refractive index and by fluorescence depolarization. Fluorescence depolarization measurements on unoriented vesicles cannot tell the difference between the orientational distributions shown in Figs. 2a and 2b. Results obtained by variation of the refractive index cannot tell the difference between the orientational distributions shown in Figs. 2b and 2c. Combining the data obtained by both techniques brought us to the conclusion that the director is possibly tilted.

It is likely that the orientation of the director coincides with the orientation of the acyl chains. Tilted orientations of the acyl chains are commonly observed in X-ray diffraction experiments [40–42]. This supports the hypothesis that the director axis Z' is tilted.

An appropriate experiment on macroscopically oriented membrane bilayers would be able to detect whether the director is normal or tilted with respect to the membrane surface. If the director is tilted, then rotating the sample around the membrane normal Z will result in varying absorption of polarized light traveling along the Z axis. The experiments on oriented membranes reported in the literature [43] were designed and interpreted with an *a priori* assumption that the orientation of the director is normal to the membrane surface. On the basis of the results obtained in these experiments one cannot decide whether the orientation of the director is normal to the membrane surface.

The second possible explanation for the discrepancy between the value of $\langle P_2(\cos\theta)\rangle$ obtained in the experiments with variable refractive index and the value of $\langle P_2(\cos\theta')\rangle$ obtained from dynamic depolarization data is that the apparent value of r_∞ measured for the membrane in its gel phase may differ from the true limit of the function $r(t)$ at $t \to \infty$. From the DPH fluorescence depolarization experiment one can obtain the value of this function only during the first 30–40 ns. The probe molecules in the gel-phase regions of the membrane may have some rotational correlation times in the range of microseconds or milliseconds. With the 10-ns lifetime of DPH fluorescence one cannot detect the slow components in the function $r(t)$. Using long-lifetime probes may give valuable additional information; however, every probe reports its own orientational order, and therefore the data obtained with different probes are not fully comparable.

Additional experimental studies with DPH in liposomes will be required to explain the difference in the value of the order parameter obtained by the different experimental techniques.

THE FOURTH-RANK ORDER PARAMETER $\langle P_4\rangle$ AND HETEROGENEITY IN THE ROTATIONAL DIFFUSION RATE $D_\perp$

Order Parameter $\langle P_4\rangle$ from Time-Resolved Emission Anisotropy

The shape of the function $r(t)$ is not involved in the determination of $\langle P_2(\cos\theta')\rangle$. Only the limit of $r(t)$ as $t \to \infty$ is important. Thus no assumption regarding the orientational dynamics in the membrane bilayer is involved in the determination of $\langle P_2(\cos\theta')\rangle$ and the results are not influenced by differing diffusion rates in different parts of the membrane.

The orientational dynamics is involved in the determination of $\langle P_4(\cos\theta')\rangle$ and if the rotational diffusion rate $D_\perp$ is the same in all parts of the bilayer, this order parameter can be determined from the shape of $r(t)$.

The equations describing the shape of the function $r(t)$ are given by Zannoni *et al.* [13]. This involves integrating the products of the Wigner rotation matrices and the Green functions obtained for the Smoluchowski rotational diffusion equation. Van der Meer *et al.* [14] approximated the solution of the model equations as a sum of three exponentials plus a constant. The approximate solution was employed as the model function that was fit to experimental data [15,16]. The rotational diffusion rate $D_\perp$ and the order parameters $\langle P_2(\cos\theta')\rangle$ and $\langle P_4(\cos\theta')\rangle$ served as fitting parameters. This allowed evaluation of the order parameter $\langle P_4(\cos\theta')\rangle$ in unoriented vesicles.

The approach to the analysis of the time-resolved anisotropy data introduced in Ref. 14 is often called model independent in the sense that the values of the order parameters $\langle P_2\rangle$ and $\langle P_4\rangle$ are determined without assuming a specific relation between them, such as the

Table I.

	Minimum No. 1			Minimum No. 2		
$D_{\perp 1}/D_{\perp 2}$	$\langle P_2 \rangle$	$\langle P_4 \rangle$	χ^2	$\langle P_2 \rangle$	$\langle P_4 \rangle$	χ^2
1.00	0.400	0.104	1.00	0.400	0.104	1.00
1.05	0.400	0.095	1.00	0.400	0.111	1.00
1.10	0.400	0.087	1.00	0.400	0.120	1.00
1.20	0.400	0.071	1.00	0.400	0.135	1.00
1.40	0.400	0.044	1.00	0.400	0.161	1.00
1.80	0.400	−0.003	1.00	0.399	0.204	1.00
2.20	0.401	−0.042	1.01	0.399	0.239	1.01
2.60	0.402	−0.071	1.06	0.399	0.268	1.01
3.00	0.404	−0.097	1.17	0.398	0.293	1.01
3.40	0.405	−0.114	1.37	0.398	0.316	1.01
3.80	0.406	−0.130	1.66	0.399	0.336	1.01
4.20	0.407	−0.143	2.06	0.399	0.355	1.01
4.60	0.409	−0.159	2.55	0.400	0.372	1.01
5.00	0.411	−0.161	3.15	0.400	0.388	1.02
5.40	0.413	−0.155	3.77	0.401	0.403	1.05
5.80	0.414	−0.154	4.50	0.403	0.417	1.09
6.20	0.416	−0.157	5.25	0.404	0.430	1.15

relations imposed by the wobbling-in-cone model [8] or Maier and Saupe model. The approach critically depends only on the assumption that the rotational diffusion rate $D_\perp$ has the same value in all parts of the membrane bilayer. The value of the order parameter $\langle P_4 \rangle$ is determined from the nonexponential behavior of $r(t)$ between r_0 and r_∞. Heterogeneity in the rotational diffusion rate would result in nonexponential anisotropy decay even in an isotropic medium. Clearly, heterogeneity in the diffusion rate will influence the recovered values of the order parameter $\langle P_4 \rangle$.

The influence of heterogeneity on the recovered values of the order parameter $\langle P_4 \rangle$ was not studied in Refs. 14–16. We performed a computer simulation to study this effect. In this simulation we assumed that there are two populations of DPH, each contributing one-half of the total fluorescence intensity. The two populations differed only in the value of the rotational diffusion rate. The ratio of the two rates $D_{\perp 1}/D_{\perp 2}$ varied from 1.0 to 6.2, while the geometric mean of the two rates was kept at the constant value of 8.33×10^7 s^{-1}, which would result in an anisotropy decay time of 2 ns in an isotropic medium. The fluorescence lifetime was 10 ns for both populations. The order parameters $\langle P_2 \rangle = 0.400$ and $\langle P_4 \rangle = 0.104$ were identical for both populations. The chosen values of the order parameters satisfy the relation imposed by the Maier and Saupe model. In the simulation we used the model equations from Ref. 14, specifically, Eq. (14) and the expressions given in Table 1 of that reference. The decay curves for the vertical and horizontal fluorescence components were convolved with the lamp profile of a Gaussian shape having 0.09-ns width at half-maximum and recorded in 2048 channels of a hypothetical multichannel analyzer having a timing calibration of 0.015 ns per channel. True-Poisson photon counting noise was added. The peak number of counts was about 10^5 for the vertical polarization component. The hypothetical experimental setup closely imitates state-of-the-art photon counting equipment employing picosecond lasers and microchannel plate photomultipliers.

In the analysis of the simulated data we used the model equations given in Ref. 14. In contrast to the simulation procedure, we assumed only one population, having a unique rotational diffusion rate $D_\perp$. This rate and the order parameters $\langle P_2 \rangle$ and $\langle P_4 \rangle$ served as the fitting parameters. The values of $r_0 = 0.4$ and $\tau = 10$ ns were fixed in the analysis. The data analysis program adjusted the values of the three fitting parameters in order to minimize the value of χ^2. Here χ^2 represents a sum of weighted squared deviations between simulated data and the model used in the analysis. The value of χ^2 is a function of $D_\perp$, $\langle P_2 \rangle$, and $\langle P_4 \rangle$; this function can be pictured as a surface in a four-dimensional space with coordinate axes $D_\perp$, $\langle P_2 \rangle$, $\langle P_4 \rangle$, and χ^2. It was found that the χ^2 surface has one or two local minima in the $\langle P_2 \rangle > 0$ subspace and at least one local minimum in the $\langle P_2 \rangle < 0$ subspace. Negative $\langle P_2 \rangle$ values are physically meaningless; we do not report the solutions obtained with $\langle P_2 \rangle < 0$. The values of the fitting parameters and χ^2 corresponding to the two minima found in the $\langle P_2 \rangle > 0$ subspace are presented in Table I. We are testing the recovery of the order parameters only; therefore the values of $D_\perp$ are not included in Table I.

The recovered values of $\langle P_4 \rangle$ and χ^2 slightly fluctuated from one data set to another. To reduce these fluctuations the results were averaged over 1000 realizations of the random noise. In other words, the simulation and the analysis was repeated 1000 times for every ratio $D_{\perp 1}/D_{\perp 2}$. The results presented in Table I are averaged. This helps to separate systematic trends from the random noise.

Each line in Table I reports the analysis of the data simulated for a certain value of the ratio $D_{\perp 1}/D_{\perp 2}$, which reflects the magnitude of heterogeneity in the hypothetical membrane. The χ^2 surface had two minima in the $\langle P_2 \rangle > 0$ subspace; both of them are presented in Table I. The two minima coincide in the case where $D_{\perp 1}/D_{\perp 2} = 1$, i.e., $D_{\perp 1} = D_{\perp 2}$, and the hypothetical membrane is perfectly homogeneous. If the values of the diffusion rates differ by as little as 5%, two separate local minima are found on the χ^2 surface. The values of the χ^2 are about the same for both minima when $0.4 < D_{\perp 1}/D_{\perp 2} <$

2.5, but when the ratio is out of this range, the value of χ^2 for the first minimum is higher than for the second one. Due to symmetrical considerations, the solution obtained for $D_{\perp 1}/D_{\perp 2} = X < 1$ is identical to the one for $D_{\perp 1}/D_{\perp 2} = 1/X$, which can be found in Table I.

The two local minima shown in Table I differ mainly in the value of $\langle P_4 \rangle$: the first minimum is characterized by low and even negative $\langle P_4 \rangle$ values, whereas the second minimum is characterized by high $\langle P_4 \rangle$ values. These are the two local minima found in the analysis of simulated data. The existence of two local minima was also discovered in the analysis of experimental data [16]. The negative $\langle P_4 \rangle$ solution corresponds to the unimodal orientational distributions shown in Fig. 8 of Wang *et al.* [16]. The positive $\langle P_4 \rangle$ solution corresponds to the bimodal orientational distributions shown in Fig. 7 of Wang *et al.* [16]. All the results reported by Ameloot *et al.* [15] correspond to the bimodal orientational distribution. Note that in the case of the bimodal distribution the value of $\langle P_4 \rangle$ is substantially greater than the values predicted with both the wobbling-in-cone model and the Maier and Saupe model. The negative and exaggerated positive $\langle P_4 \rangle$ values can be real or alternatively they could result from the heterogeneity in the rotational diffusion rate. As can be seen from Table I, when the ratio $D_{\perp 1}/D_{\perp 2}$ is within the range from 0.2 to 5, the heterogeneity in the rotational diffusion rate results in an anisotropy decay which is practically indistinguishable from the one obtained in the case of exaggerated $\langle P_4 \rangle$ values. This does not prove that the interpretations in Refs. 15 and 16 are wrong; however, one should consider the possibility of the alternative interpretation based on the heterogeneity in the diffusion rate constant.

The results reported in Refs. 15 and 16 were obtained with synthetic membranes which do not exhibit domain structure; therefore there was no reason to invoke heterogeneity in the interpretation of these data. Natural membranes and the synthetic membranes prepared from mixtures of phospholipids often exhibit domain structure. Since rotational diffusion rates differ in liquid and gel domains it will be difficult to obtain $\langle P_4 \rangle$ in heterogeneous membranes.

Detection of Microheterogeneity by Time-Resolved Fluorescence Anisotropy of DPH

Interpretation of time-resolved fluorescence anisotropy data critically depends on whether the population of DPH in the membrane is homogeneous or heterogeneous. Even a slight heterogeneity in the rotational diffusion rate would interfere with the determination of the order parameter $\langle P_4 \rangle$. Presence of the gel phase can also influence the value of the order parameters $\langle P_2 \rangle$ determined from the limiting anisotropy. In this connection it is important to be able to detect heterogeneity in the DPH environment.

Multiexponential decay of the total fluorescence intensity of DPH was attributed to the heterogeneity in its environment [29–34]; however, there are several other explanations for the multiexponential decay of this probe [25–28,35,36]. Complex fluorescence anisotropy decay cannot serve as a proof of membrane heterogeneity either, because complex anisotropy decay is expected in an anisotropic environment. There is one case where the fluorescence anisotropy decay of DPH can serve as a reliable proof of the heterogeneity of its environment. This is the case where after a rapid initial decrease the time-resolved anisotropy $r(t)$ starts to increase with time. The mechanism of such behavior is considered below.

For a fluorescent probe with parallel or near-parallel orientations of the absorption and emission dipole the time-resolved anisotropy in any homogeneous environment, either isotropic or anisotropic, must be a monotonously decreasing function of time. If the membrane has multiple environments $j = 1,2, \ldots$, then the local anisotropy $r_j(t)$ in each environment must be a monotonously decreasing function. If the fluorescence intensity decay is identical in all environments, then the anisotropy of the mixture equals the sum of the individual anisotropies multiplied by their fractional intensity contributions:

$$r(t) = \sum f_j r_j(t) \tag{14}$$

If the local anisotropy $r_j(t)$ in each environment is a monotonously decreasing function, then the global anisotropy $r(t)$ predicted by Eq. (14) will be a monotonously decreasing function. The situation changes in the case where the fluorescence intensity decay is different in different environments. In this case instead of Eq. (14) we have to use the following:

$$r(t) = \frac{\sum I_j(t)\, r_j(t)}{\sum I_j(t)} \tag{15}$$

For simplicity we can assume that the membrane has only two environments, $j = 1,2$, the first environment being the gel phase and the second one being the liquid phase. It is well known that the fluorescence lifetime of DPH in the gel phase is slightly longer than in the liquid phase [29–31]. It is also well known that the value of the asymptotic term r_∞ in the gel phase is greater than in the liquid phase [5–7]. During the first few nanoseconds the local anisotropies $r_j(t)$ decrease

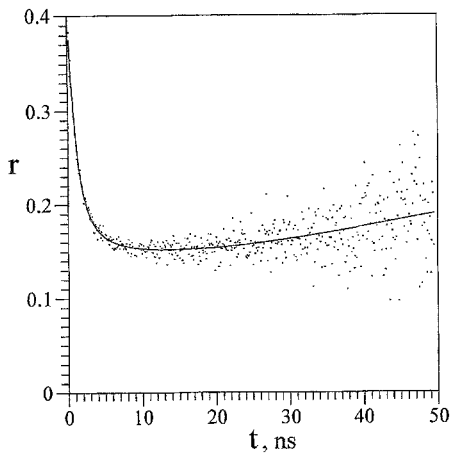

Fig. 3. Time-resolved anisotropy of DPH in DPPC large unilamellar vesicles at 40°C. The results of the analysis of these data can be found in Table 1 in Ref. 35. Dots: $r(t)$ calculated from the experimental data as $(I_{\parallel} - I_{\perp}) / (I_{\parallel} + 2I_{\perp})$. Curve: exponential series fit to the $r(t)$ data.

from the value of r_0 to the local $r_{j\infty}$ values. After the end of this initial period the behavior of the global anisotropy is driven by the slow redistribution of the fluorescence intensity between the two populations rather than by the variations in the local anisotropies $r_j(t)$. The fractional contribution of the gel phase increases with time; therefore the value of the global anisotropy $r(t)$ will increase, too.

If the lifetime of DPH is about 11 ns in the gel phase and about 9 ns in the liquid phase, then the difference $r_{1\infty} - r(t)$ will decay to zero at the rate of $1/9 - 1/11 \approx 0.02$ ns^{-1}, which corresponds to the decay time of 50 ns. One cannot observe $r(t)$ reaching the $r_{1\infty}$ limit, because fluorescence intensity decays faster than the difference $r_{1\infty} - r(t)$. In the experiment one can see only the beginning of this slow process; therefore the observed increase in $r(t)$ will be very small. Figure 3 shows the behavior of $r(t)$ calculated from the experimental data reported in Ref. 35. The results reported in Table 1 in this reference were obtained from the analysis of these data. The data shown in Fig. 3 were obtained with DPH in DPPC vesicles at the temperature of 40°C, which is close to the midpoint of the phase transition temperature of DPPC. At the temperatures far away from the phase transition of the lipid the increase in $r(t)$ was not observed. It is likely that at the latter temperatures the membrane is homogeneous.

The increase in $r(t)$ has been observed with paranaric acid under the conditions where both liquid and gel phase were present [44,45]. It is likely that the increase in $r(t)$ can be observed with any probe that has different fluorescence lifetimes in the gel and liquid phases. The increase is observed only when the gel and liquid phases are present in significant quantities. Unfortunately, the proposed test is not sensitive enough to detect a small fraction of the minor phase; therefore the absence of the increase in $r(t)$ cannot serve as a proof of homogeneity.

SUMMARY

Determination of the order parameters from fluorescence depolarization and resolving microenvironments in lipid membranes are closely related subjects. The method for measuring the order parameter $\langle P_4 \rangle$ in unoriented vesicles may give incorrect results if the rotational diffusion rate is slightly different in different parts of the membrane. The determination of the order parameter $\langle P_2 \rangle$ is independent of the membrane heterogeneity until the membrane is free from the gel phase. In membranes where the gel phase is present the value of the order parameter $\langle P_2 \rangle$ obtained from the long-time limit of the time-resolved anisotropy can be significantly higher than the actual value. The effects of membrane heterogeneity on the recovery of the order parameters has not been studied adequately. This opens a wide field for future investigations.

ACKNOWLEDGMENT

This work is supported by NIH Grant No. GM 11632.

REFERENCES

1. M. Shinitzky, A.-C. Dianoux, C. Gitler, and G. Weber (1971) *Biochemistry* **10**, 2106–2113.
2. U. Cogan, M. Shinitzky, G. Weber, and T. Nishida (1973) *Biochemistry* **12**, 521–528.
3. M. Shinitzky and Y. Barenholz (1974) *J. Biol. Chem.* **249**, 2652–2657.
4. F. Perrin (1929) *Ann. Phys.* (Paris) **121**, 168–275.
5. L. A. Chen, R. E. Dale, S. Roth, and L. Brand (1977) *J. Biol. Chem.* **252**, 2163–2169.
6. R. E. Dale, L. A. Chen, and L. Brand (1977) *J. Biol. Chem.* **252**, 7500–7510.
7. S. Kawato, K. Kinosita, Jr., and A. Ikegami (1977) *Biochemistry* **16**, 2319–2324.
8. K. Kinosita, Jr., S. Kawato, and A. Ikegami (1977) *Biophys. J.* **20**, 289–305.
9. M. P. Heyn (1979) *FEBS Lett.* **108**, 359–364.
10. F. Jähnig (1979) *Proc. Natl. Acad. Sci. USA* **76**, 6361–6365.
11. G. Lipari and A. Szabo (1980) *Biophys. J.* **30**, 489–506.
12. C. Zannoni (1981) *Mol. Phys.* **42**, 1303–1320.
13. C. Zannoni, A. Arcioni, and P. Cavatorta (1983) *Chem. Phys. Lipids* **32**, 179–250.

14. W. van der Meer, H. Pottel, W. Herreman, M. Ameloot, H. Hendrickx, and H. Schröder (1984) *Biophys. J.* **46**, 515–523.
15. M. Ameloot, H. Hendrickx, W. Herreman, H. Pottel, F. V. Cauwelaert, and W. van der Meer (1984) *Biophys. J.* **46**, 525–539.
16. S. Wang, J. M. Beechem, E. Gratton, and M. Glaser (1991) *Biochemistry* **30**, 5565–5572.
17. L. Davenport, J. R. Knutson, and L. Brand (1986) *Biochemistry* **25**, 1811–1816.
18. M. Shinitzky and Y. Barenholz (1978) *Biochem. Biophys. Acta* **515**, 367–394.
19. R. H. Bisby, R. B. Cundall, L. Davenport, I. D. Johnson, and E. W. Thomas (1981) in G. S. Beddard and M. A. West (Eds.), *Fluorescent Probes*, Academic Press, San Diego, pp. 97–111.
20. B. R. Lentz (1988) in L. M. Loew (Ed.), *Spectroscopic Membrane Probes*, Vol. 1, CRC Press, Boca Raton, Florida, Chapter 2, pp. 13–41.
21. B. R. Lentz (1993) *Chem. Phys. Lipids* **64**, 99–116.
22. A. N. Nikitin, M. D. Galanin, G. S. Ter-Sarkisian, and B. M. Mikhailov (1959) *Opt. Spectrosc.* **6**, 226–230.
23. E. D. Cehelnic, R. B. Cundall, J. R. Lockwood, and T. F. Palmer (1975) *J. Phys. Chem.* **79**, 1369–1376.
24. S. J. Strickler and R. A. Berg (1962) *J. Chem. Phys.* **37**, 814–822.
25. J. B. Birks and D. J. Dyson (1963) *Proc. R. Soc. Lond. A* **275**, 135–148.
26. K. Schulten and M. Karplus (1972) *Chem. Phys. Lett.* **14**, 305–309.
27. B. S. Hudson and B. E. Kohler (1973) *J. Chem. Phys.* **59**, 4984–5002.
28. J. B. Birks and D. J. S. Birch (1975) *Chem. Phys. Lett.* **31**, 608–610.
29. R. D. Klausner, A. M. Kleinfeld, R. L. Hoover, and M. J. Krasnovsky (1980) *J. Biol. Chem.* **255**, 1286–1295.
30. D. A. Barrow and B. R. Lentz (1985) *Biophys. J.* **48**, 221–234.
31. T. Parasassi, F. Conti, M. Glaser, and E. Gratton (1984) *J. Biol. Chem.* **259**, 14011–14017.
32. R. M. Forini, M. Valentino, S. Wang, M. Glaser, and E. Gratton (1987) *Biochemistry* **26**, 3864–3870.
33. B. R. Lentz and S. W. Burgess (1989) *Biophys. J.* **56**, 723–733.
34. T. Parasassi, G. De Stasio, R. M. Rusch, and E. Gratton (1991) *Biophys. J.* **59**, 466–475.
35. D. Toptygin, J. Svobodova, I. Konopasek, and L. Brand (1992) in *Time-Resolved Laser Spectroscopy in Biochemistry III*, SPIE **1640**, pp. 739–751.
36. D. Toptygin, J. Svobodova, I. Konopasek, and L. Brand (1992) *J. Chem. Phys.* **96**, 7919–7930.
37. W. Lukosz (1980) *Phys. Rev. B* **22**, 3030–3038.
38. D. Toptygin and L. Brand (1993) *Biophysical Chemistry* **48**, 205–220.
39. E. Gratton and T. Parasassi, *J. Fluorescence*, this issue.
40. M. J. Janiak, D. M. Small, and G. G. Shipley (1976) *Biochemistry* **15**, 4575–4580.
41. J. Katsaras, D. S-C. Yang, and R. M. Epand (1992) *Biophys. J.* **63**, 1170–1175.
42. S. Tristram-Nagle, R. Zhang, R. M. Suter, C. R. Worthington, W.-J. Sun, and J. F. Nagle (1993) *Biophys. J.* **64**, 1097–1109.
43. R. P. H. Kooyman, M. H. Vos, and Y. K. Levine (1983) *Chem. Phys.* **81**, 461–472.
44. A. Ruggiero and B. Hudson (1989) *Biophys. J.* **55**, 1111–1124.
45. A. Ruggiero and B. Hudson (1989) *Biophys. J.* **55**, 1125–1135.